Reducing the Ecotoxicity of Pesticide Polluted Waters by Electrochemical Methods

CRISTIAN NEAMTU, BOGDAN TUTUNARU*, ADRIANA SAMIDE, ALEXANDRU POPESCU
University of Craiova, Faculty of Sciences, Department of Chemistry, 107i Calea Bucuresti,Craiova, Romania

Electrochlorination constitutes an electrochemical approach for the treatment of pesticide-containing wastewaters. This study evaluated the electrochemical and thermal stability of four pesticides and the efficiency of electrochlorination to remove and detoxify the simulated polluted water with: Acetamiprid, Emamectin, Imidacloprid and Propineb. This study reports the experimental results obtained by cyclic voltammetry and electrolysis at constant current density in association with UV-Vis spectrophotometry. In saline waters this pesticides are electrochemical active and anodic peaks are registered in the corresponding voltammograms. After thermal combustion, in a gaseous nitrogen atmosphere, a residue ranging from 15 to 45 % is observed at 500 °C.

Keywords: pesticide, electrochemistry, spectrophotometry, thermochemistry

The agricultural management use pesticides for pest control and to assure food quality and quantity. A large amount of insecticides, herbicides and fungicides didn‘t reaches their purpose and results in a negative impacts on ecosystems [1, 2]. Currently used pesticides, especially organochloride ones are resistant to conventional treatment methods and due to their low physico-chemical degradability, low aqueous solubility and low biodegradability. Acute and chronic toxic effects of pesticides or their metabolites on biological species were demonstrated [3, 4].

Biosensors are one of the most used tools for pesticide detection or quantification. Biosensors based on acetylcholinesterase (AChE) enzyme immobilization on sol-gel Zn-O matrix were used for amperometric detection of paraoxon [5]. Voltammetric or amperometric detection of chlorpyriphos and triazophos using AChE biosensor based on carbon nanostructure - chitosan matrix showed increased detection sensitivity [6, 7]. Electrochemical detection of dichlorophen, carbaryl, methomyl, paraoxon-methyl, fenitrothion and chlorpyrifos with biosensors based on composite matrix of carbon nanotubes and conducting polymers was studied [8-10].

The development of new electrodes, such as TiO_2/Ti nanotubes [11], graphene oxide composite film [12] and carbon paste transducer [13] have been used to study the electrochemical behavior of thiamethoxam, methyl parathion and fenitrothion respectively.

Enzymatic and non-enzymatic sensors based on Au, Ag, Pt, ZrO_2 and α-Al_2O_3 nanoparticles have been used for electrochemical study of pesticides [14-20]. Mineralization of glyphosate, malathion, bazudin, chlorophos, methaphos, chloropyriphos, demethon, metamidophos, fenthion, diazinon have been carried out using different metallic electrodes [21-25].

The objective of this study was to reduce the ecotoxicity of four commercial pesticides currently used in agricultural practices. Using electrochemical methods, acetamiprid, emamectin, imidacloprid and propineb were analysed in order to study their electrochemical degradation in chloride solution under constant current density. This paper presents the experimental results of electrochemical and thermal degradation of four common used pesticides.

Experimental part

Materials and methods

Aqueous test solutions of 10^{-4} mol·L^{-1} acetamiprid, 10^{-5} mol·L^{-1} emamectin, 10^{-4} mol·L^{-1} imidacloprid and $5\cdot10^{-4}$ mol·L^{-1} propineb containing 10^{-1} mol·L^{-1} NaCl as supporting electrolyte were prepared. NaCl was purchased from Sigma-Aldrich and the pesticides were purchased by a local commercial supplier. The trade name, concentration and the molecular structure of the used pesticides are presented in table 1.

Cyclic voltammetry and electrolysis at constant current density were performed with a VoltaLab 40 electrochemical system equipped with VoltaMaster 4 software in order to study the electrochemical bahavior and electrochemical degradation of four commercial pesticides; acetamiprid, emamectin, imidacloprid and propineb.

A conventional three-electrode one compartment electrochemical cell was used. Platinum plates (Pt 99.999 %, 2 cm^2 active surface) were used as anode and cathode and a silver chloride electrode (KCl saturated) it served as reference.

Cyclic voltammetric measurements were performed under dynamic condition (agitation, stirring rate = 300 rpm) between -2.0 V and +2.0 V at a scan rate of 100 mV·s^{-1}.

The electrochemical mineralization of the pesticides was performed at a constant current density of 50 mA·cm^{-2} in dynamic conditions of agitation. All electrochemical measurements were performed at room temperature.

UV-Vis spectra of electrolized solution were registered at different times of electrolysis with a Varian Cary spectrophotometer equipped with a 1 x 1 x 4.5 cm quartz cell.

Thermal behaviour of the pesticides was studied by a Perkin Elmer thermal analyser (Pyris software) between room temperature and 500°C. Thermal analysis as thermogravimetry (TG) and differential scanning calorimetry (DSC) were performed in inert nitrogen atmosphere (150 mL· min^{-1}) with a heating rate of 10°C·min^{-1}. Both reference and working crucibles were made from aluminium.

---

* *email: tutunaruchim@yahoo.com*

Table 1
THE COMMERCIAL PESTICIDES TREATED BY ELECTROCHEMICAL METHODS

Trade name	Active component	Concentration	Molecular structure
Mospilan	Acetamiprid	20 %	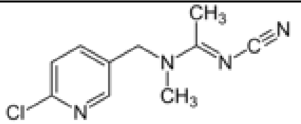
Affirm	Emamectin	0.95 %	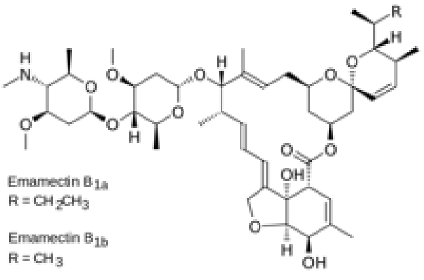 Emamectin B_{1a} $R = CH_2CH_3$ Emamectin B_{1b} $R = CH_3$
Sojet	Imidacloprid	10 %	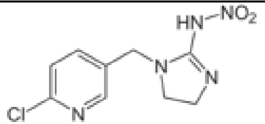
Antracol	Propineb	70 %	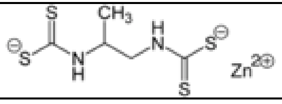

Results and discussions

Electrochemical and thermal degradation of acetamiprid

In figure 1 are presented the cyclic voltamograms of platinum electrode in 10^{-1} mol·L^{-1} NaCl solution both in the absence and in the presence of 10^{-4} mol·L^{-1} acetamiprid. By representing the voltamograms (fig. 1a) and the details corresponding to the low values of the current densities (fig. 1b), two significant differences are identified:

-three peaks of cathodic current densities corresponding to the electrochemical reduction of the active species of chlorine are observed in the absence of pesticide molecules;

-In the presence of pesticide molecules an anodic peak is recorded at the 1.35 V value of the working electrode potential, most probably attributed to the pesticide molecules oxidation at the electrode surface.

UV-Vis spectrophotometry analysis shows an absorbance peak in the Vis domain (λ = 630 nm) for high values of pesticide concentrations (10^{-2} mol·L^{-1}) (fig. 2.a). During electrolysis at constant current density (i = 50 mA·cm^{-2}) there is a very low decrease in the initial absorbance.

At lower values of the pesticide concentration (10^{-4} mol·L^{-1}) a maximum absorption corresponding to the wavelength of 250 nm is recorded (fig. 2.b).

By recording the UV-Vis spectra of the electrolyzed solution, a new absorption peak (λ = 290 nm) is observed which shows increasing absorption values over time. The appearance of this new absorption peak indicates the presence / formation of a new compound whose concentration increases with time and this compound may be the final or intermediate product of pesticide electrochemical degradation.

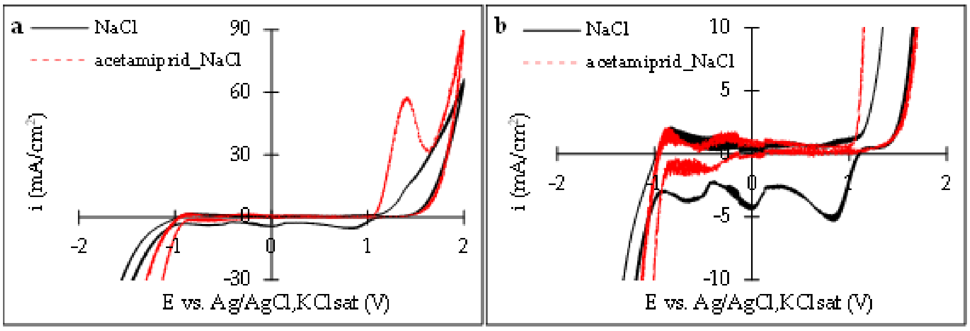

Fig. 1. Cyclic voltammograms of Pt electrode in 10^{-1} mol·L^{-1} NaCl solution, in the absence and in the presence of 10^{-4} mol·L^{-1} acetamiprid pesticide, 100 mV·s^{-1}

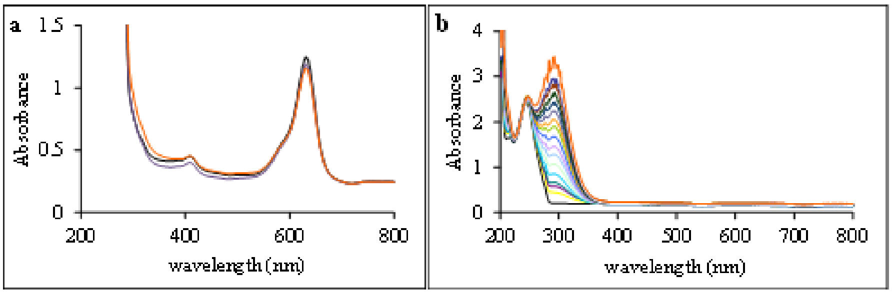

Fig. 2. UV-Vis spectra of 10^{-4} mol·L^{-1} acetamiprid, 10^{-1} mol·L^{-1} NaCl solution; initially and at different electrolysis times (10 to 10 mins.)

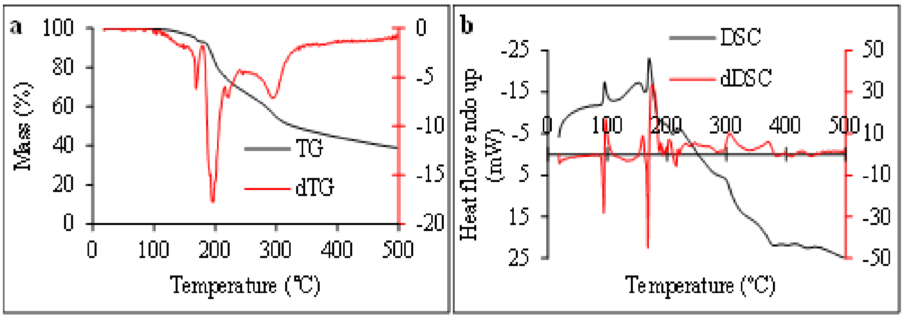

Fig. 3. The TG/dTG and DSC/dDSC thermograms of acetamiprid, 10 °C·min^{-1}

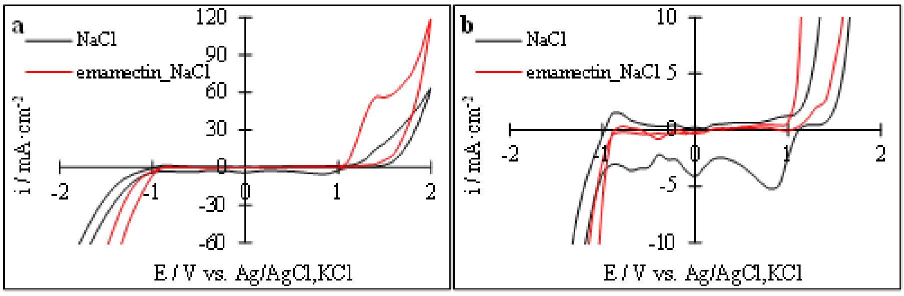

Fig. 4. Cyclic voltammograms of Pt electrode in 10^{-1} mol·L^{-1} NaCl solution, in the absence and in the presence of 10^{-5} mol·L^{-1} emamectin, 100 mV·s^{-1}

According to the TG / DSC thermograms shown in Figure 3 (3.a and 3.b), it is observed that a first thermal effect is recorded at a temperature of 94 °C and is attributed to the melting point of the pesticide (98.9 °C).

Thermal degradation of acetamiprid occurs in several successive steps as follows:

- 120 ÷ 170 ° C; weight loss ~ 10%;
- 170 ÷ 210 ° C; weight loss ~ 20%;
- 210 ÷ 300 ° C; weight loss ~ 20%;
- 300 ÷ 500 ° C; weight loss ~ 10%;

At the end of the experiment, at a temperature of 500 °C, a residue of about 40 % remains in the crucible.

Electrochemical and thermal degradation of emamectin

Figure 4 shows the cyclic voltamograms of platinum electrode in 10^{-1} mol·L^{-1} NaCl solution both in the absence and in the presence of 10^{-5} mol·L^{-1} emamectin pesticide.

At potentials values of the working electrode greater than 1.0 V, the two voltamograms differ significantly. A new maximum of current density (1.3 V vs Ag / AgCl) is recorded and at the same time there is an intensification of the charge transfer processes at the metal / electrolyte interface when the pesticide molecules are present in the electrolyte solution (fig. 4).

At negative or low positive values of the working electrode potentials it is noted that the current densities of the voltammogram registered in the presence of pesticide molecules has lower values than those corresponding to the supporting electrolyte, this being due to strong adsorption of pesticide molecules on the surface of the electrode.

Emamectin molecules are photolytic active in the UV field, exhibiting a maximum absorbance at the wavelength of 228 nm.

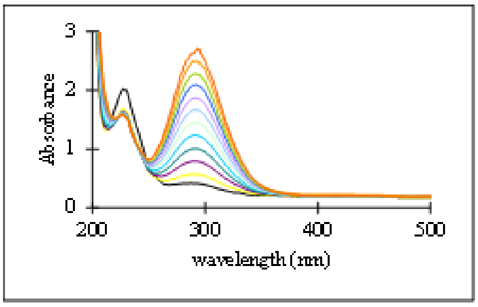

Fig. 5. UV-Vis spectra of 10^{-5} mol·L^{-1} emamectin, 10^{-1} mol·L^{-1} NaCl solution; initially and at different electrolysis times (2 to 2 mins.)

The UV-Vis spectra of the electrolyte solution containing 10^{-5} mol·L^{-1} emamectin recorded at different electrolysis times indicates a decrease in emamectin absorbance values while a new peak of absorbance is registered (λ = 290 nm). This absorbance peak, recorded at the wavelength of 290 nm, is most likely attributed to the formation of an intermediate compound of the emamectin molecule degradation.

Figure 6 shows the TG / dTG / DSC / dDSC thermograms of emamectin. According to the TG / dTG curves (fig. 6.a) it is observed that thermal degradation of emamectin takes place in several successive stages; a first thermal effect is recorded at a temperature of 150 °C associated with a 5 % decrease in mass; the second degradation step registered in the range of 215 °C ÷ 260 °C associated with a 20 % of mass loss; the third degradation step is in the range 260 °C ÷ 320 °C associated with a 30 % decrease in mass; the fourth degradation step observed in the range of 260 °C ÷ 500 °C associated with a 15 % decrease of mass.

At the end of the experiment (500 °C) a residue of about 30 % is recorded.

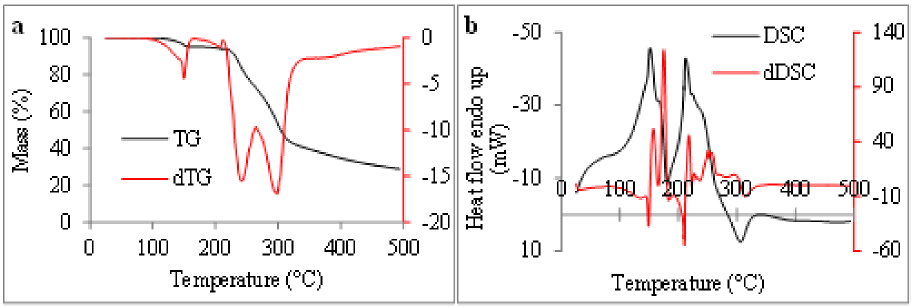

Fig. 6. The TG/dTG and DSC/dDSC thermograms of emamectin, 10 °C·min^{-1}

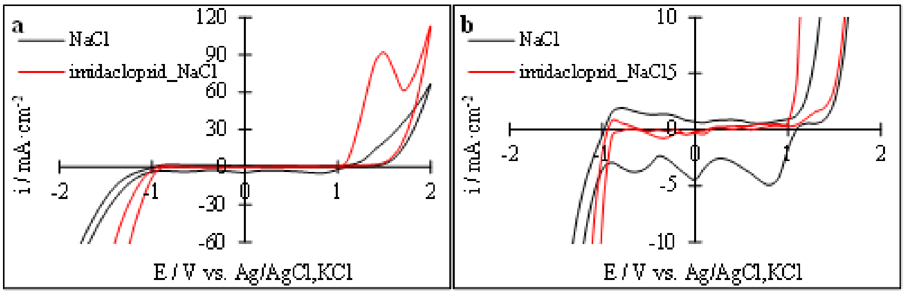

Fig. 7. Cyclic voltammograms of Pt electrode in 10^{-1} mol·L^{-1} NaCl solution, in the absence and in the presence of 10^{-4} mol·L^{-1} imidacloprid, 100 mV·s^{-1}

Electrochemical and thermal degradation of imidacloprid

Figure 7 shows the cyclic voltamograms of platinum electrode in 10^{-1} mol·L^{-1} NaCl solution both in the absence and presence of imidacloprid in a concentration of 10^{-4} mol·L^{-1}.

The imidacloprid molecules exhibit electrochemical behavior similar to the two previously studied pesticides (acetamiprid and emamectin, respectively). A new peak of anode current densities is identified (fig. 7.a) at a working electrode potential of approximately 1.5 V vs. Ag/AgCl, associated with electrochemical oxidation of pesticide molecules.

In the potentials range -1.0 ÷ +1.0 V, the current densities recorded in the presence of organic molecules of imidacloprid show lower values than those recorded only in the presence of the support electrolyte. This demonstrates the participation of pesticide molecules in electrode processes associated with a decrease in electronic transfer rate at the metal / electrolyte solution interface.

The imidacloprid molecules are active in the UV domain and are characterized by a maximum of absorbance at a wavelength of 270 nm (fig. 8).

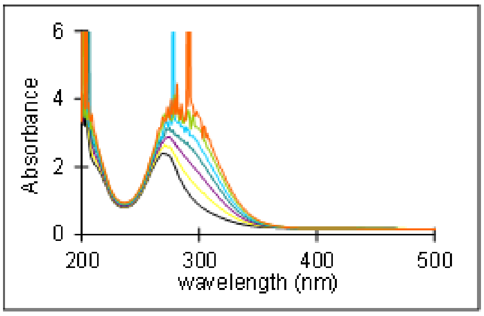

Fig. 8. UV-Vis spectra of 10^{-4} mol·L^{-1} imidacloprid, 10^{-1} mol·L^{-1} NaCl solution; initially and at different electrolysis times (5 to 5 mins.)

Figure 8 shows the UV-Vis spectra recorded at different electrolysis times of the electrolyte solution containing 10^{-5} mol·L^{-1} emamectin and indicates the increase of absorbance values corresponding to λ = 270 nm.

This maximum absorbance at the wavelength of 270 nm is most likely attributable to the formation of an intermediate compound of the emamectin molecule degradation. Characteristic of this absorption maximum is that the absorbance values increase over time and at the same time there is a shift of the maximum to higher wavelengths (from λ = 270 nm to λ= 290 nm).

Figure 9 shows the TG / dTG / DSC / dDSC thermograms of imidacloprid. According to the TG / dTG curves (fig. 9a) it is observed that thermal degradation takes place in several successive stages; a first thermal effect is recorded in the range of 75 °C ÷ 200 °C associated with a 5 % decrease in mass; the second degradation step is recorded in the range of 200 °C ÷ 300 °C associated with a 45 % of mass loss; the third degradation step is in the 300 °C ÷ 500 °C range associated with a 15 % decrease in mass.

At the end of the experiment (500 °C), a residue of approximately 35 % remains in the crucible.

Electrochemical and thermal degradation of propineb

Figure 10 shows the cyclic voltammograms of platinum electrode in 10^{-1} mol·L^{-1} NaCl solution in the absence and presence of $5\cdot10^{-4}$ mol·L^{-1} propineb.

The current densities of the voltammogram registered in the presence of pesticide molecules has lower values than those corresponding to the supporting electrolyte, this demonstrates that the charge transfer processes take place by the initial adsorption of the pesticide molecules on the surface of the electrode.

By making a detail of cyclic voltamograms at low values of current densities, a new maximum of the current densities associated with electrooxidation of pesticide molecules is more easily identified. This process is also demonstrated by recording UV-Vis spectrophotograms.

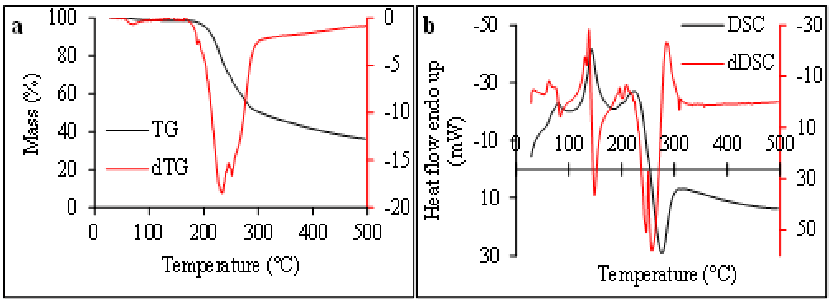

Fig. 9. The TG/dTG and DSC/dDSC thermograms of imidacloprid, 10 °C·min^{-1}

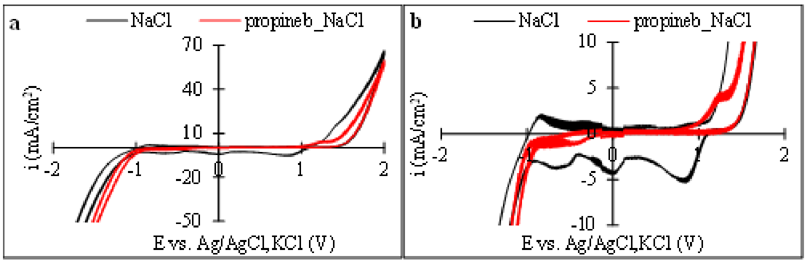

Fig. 10. Cyclic voltammograms of Pt electrode in 10^{-1} mol·L^{-1} NaCl solution, in the absence and in the presence of 10^{-4} mol·L^{-1} propineb, 100 mV·s^{-1}

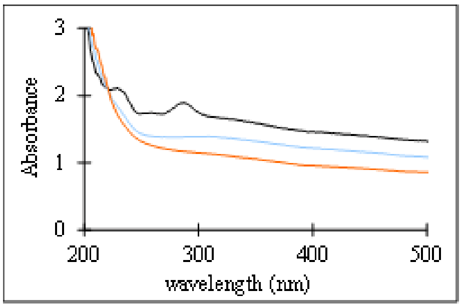

Fig. 11. UV-Vis spectra of 10^{-5} mol·L^{-1} propineb, 10^{-1} mol·L^{-1} NaCl solution; initially and at different electrolysis times (10 to 10 mins.)

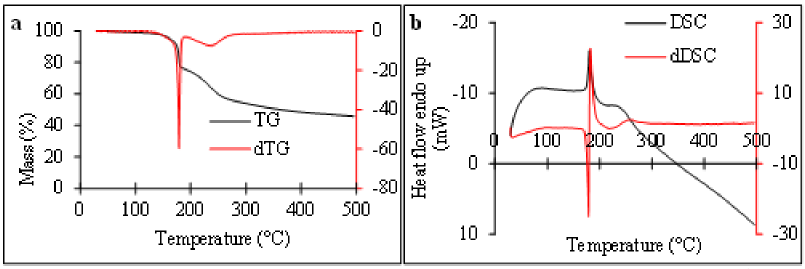

Fig. 12. The TG/dTG and DSC/dDSC thermograms of propineb, 10 °C·min^{-1}

Figure 11 shows the UV-Vis spectra of $5 \cdot 10^{-4}$ mol·L^{-1} Propineb, 10^{-1} mol·L^{-1} NaCl solution at different times from the start of the electrolysis process; 0 min (start) and after 20 and 40 min respectively after the start of the electrolysis process.

In the UV field, propineb molecules are active, exhibiting two absorption peaks corresponding to wavelengths λ = 230 nm and λ = 287 nm. During electrolysis processes, propineb molecules are electrochemically degraded; so that the absorbance values of propineb decrease over time. According to figure 11, it can be concluded that after 40 minutes of electrolysis initiation, electrochemical degradation of propineb is complete.

An important feature of propineb electrochemical degradation, unlike the behavior of the other three pesticides studied, is that propineb does not form other intermediate degradation products.

Thermogravimetric (TG) and Differential Scanning Calorimetric (DSC) curves, respectively their derivatives (dTG and dDSC), show a thermal degradation of propineb in two steps, as follows: in the temperature range 140 ÷ 180 °C the first mass loss of about 25 %, and in the 180 ÷ 260 °C temperature range, the second mass loss of 20 % is recorded. At temperatures higher than 260 °C (260 ÷ 500 °C), a slow mass loss of 10 % is recorded.

At the end of the experiment (500 °C), a residue of approximately 45 % remains in the crucible.

Conclusions

By recording the cyclic voltamograms of the four studied pesticides it is observed that the they presents anode oxidation maxima, which most probably are attributed to the electrooxidation of pesticides, meaning they are electrochemically active.

Spectrophotometric analysis of electrolyzed solutions at constant current density shows that 3 compounds (acetampirid, emamectin and imidacloprid) form new absorption maxima attributed to the formation of new compounds, and in the case of propineb there is a decrease in corresponding absorbances, indicating that degrades electrochemically without forming intermediate products.

From the thermal analysis, the interpretation of the TG / DTG / DSC thermograms shows that all compounds degraded at several temperature ranges.

References

1. HVEZDOVA, M., KOSUBOVA, P., KOSIKOVA, M., SCHERR, K.E., SIMEK, Z., BRODSKY, L., SUDOMA, M., SKULCOVA, L., SANKA, M., SVOBODOVA, M., KRKOSKOVA, L., VASICKOVA, J., NEUWIRTHOVA, N., BIELSKA, L., HOFMAN, J., Sci. Total Environ., 613–614, 2018, p. 361.
2. JING, L., BING, C., WEN, D., ZHENG, J., ZHANG, B., J. Environ. Manag., 203, part 1, 2017, p. 182.
3. LIZANO-FALLAS, V., MASIS-MORA, M., ESPINOZA-VILLALOBOS, D., LIZANO-BRENES, M., RODRIGUEZ-RODRIGUEZ, C.E., Chemosphere, 182, 2017, p. 106.
4. KIM, S.Y., AHM, H.G., HA, P.J., LIM, U.T., LEE, J.-H., J. Asia-Pac. Entomol., 21, no. 1, 2018, p. 1.
5. SINHA, R., GANESANA, M., ANDREESCU, S., STANCIU, L., Analyt. Chim. Acta, 661, no. 2, 2010, p. 195.
6. DU, D., HUANG, X., CAI, J., ZHANG, A., Sensor. Actuat. B-Chem., 127, no. 2, 2007, p. 531.
7. ION, I., ION, A.C., Mat. Sci. Eng. C-Mater, 32, no. 4, 2012, p. 1001.
8. SGOBBI, L.F., MACHADO, S.A.S., Biosens. Bioelectron., 100, 2018, p. 290.
9. CESARINO, I., MORALES, F.C., LANZA, M.R.V., MACHADO, S.A.S., Food Chem., 135, 2012, p. 873.
10. SIPA, K., BRYCHT, M., LENIART, A., URBANIAK, P., NOSAL-WIERCINSKA, A., PALECZ, B., SKRZYPEK, S., Talanta, 176, 2018, p. 625.
11. MAULIDIYAH, AZIZ, T., NURWAHIDAH, A.T., WIBOWO, D., NURDIN, M., Environmental Nanotechnology, Monitoring & Management, 8, 2017, p. 103.
12. LIU, G., LIN, Y., Electrochem. Commun., 7, no. 4, 2005, p. 339.
13. SURUCU, O. BOLAT, G., ABACI, S., Talanta, 168, 2017, p. 113.
14. GULER, M., TURKOGLU, V., BASI, Z., Electrochim. Acta, 240, 2017, p. 129.
15. JIRASIRICHOTE, A., PUNRAT, E., SUEA-NGAM, A., CHAILAPAKUL, O., CHUANUWATANAKUL, S., Talanta, 175, 2017, p. 331.
16. HUIXIANG, W., DANQUN, H., YANAN, Z., NA, M., JINGZHOU, H., MIAO, L., CAIHONG, S., CHANGJUN, H., Sensor. Actuat. B-Chem., 252, 2017, p. 1118.
17. MALARKODI, C., RAJESHKUMAR, S., ANNADURAI, G., Food Control, 80, 2017, p. 11.
18. GONG, J., WANG, L., MIAO, X., ZHANG, L., Electrochem. Commun., 12, no. 11, 2010, p. 1658.
19. WEI, Y., XU, R.-X., GAO, C., LIU, J.-H., HUANG, X.-J., Electrochem. Commun., 18, 2012, p. 78.
20. DU, D., YE, X., ZHANG, J., ZENG, Y., TU, H., ZHANG, A., LIU, D., Electrochem. Commun., 10, no. 5, 2008, p. 686.
21. KUKURINA, O., ELEMESOVA, Z., SYSKINA, A., Procedia Chem., 10, 2014, p. 209.
22. SAMET, Y., AGENGUI, L., ABDELHEDI, R., J. Electroanal. Chem., 650, no. 1, 2010, p. 152.
23. VLYSSIDES, A., ARAPOGLOU, D., MAI, S., BARAMPOUTI, E.M., Chemosphere, 58, 2005, p. 439.
24. CHENG, X., WANG, Q., ZHANG, S., ZHANG, W., HE, P., FANG, Y., Talanta, 71, 2007, p. 1083.
25. AKYUZ, D., KELES, T., BIYIKLIOGLU, Z., KOCA, A., J. Electroanal. Chem., 804, 2017, p. 53.

Manuscript received: 10.05.2018